J Am Soc Nephrol 9: 1464–1473, 1998

Heparin-Binding EGF-Like Growth Factor mRNA Is Upregulated in the Peri-Infarct Region of the Remnant Kidney Model: *In Vitro* Evidence Suggests a Regulatory Role in Myofibroblast Transformation

GEOFFREY KIRKLAND,* KATHY PAIZIS,* LEONARD L. WU,†
MARINA KATERELOS,* and DAVID A. POWER*

**Departments of Clinical Immunology and Nephrology, St. Vincent's Hospital, Fitzroy, Victoria, Australia; and *Department of Medicine, University of Melbourne, Austin & Repatriation Medical Centre, West Heidleberg, Victoria, Australia.*

Abstract. Heparin-binding epidermal growth factor-like growth factor (HB-EGF) is a potent fibroblast and epithelial cell mitogen that may be important in wound healing. The aim of this study was to determine its distribution and possible function in segmental renal infarction. At day 1 postinfarction, *in situ* hybridization showed that HB-EGF mRNA was markedly increased by tubular epithelial cells bordering the infarcted zone. At day 3, typical myofibroblasts expressing α-smooth muscle actin (α-SMA) were present in large numbers at the peri-ischemic border and, over succeeding days, were also seen within the infarcted area. Some of these cells expressed HB-EGF mRNA by *in situ* hybridization suggesting possible autocrine stimulation. Endothelial cells appeared to be more resistant to ischemia than tubules because some capillaries at the periphery of the infarct, surrounded by infarcted tubules, also expressed HB-EGF mRNA. The staining intensity of HB-EGF mRNA in individual tubules and endothelial cells was maximal at day 5 after infarction, although Northern blots of tissue from the peri-infarct area only showed significantly increased expression of HB-EGF mRNA at days 1 and 3, perhaps reflecting a smaller area of greater intensity of expression at day 5. Because tubular cells expressing high levels of HB-EGF mRNA were directly apposed to myofibroblasts, an attempt was made to determine whether HB-EGF contributed to upregulation of α-SMA by human fibroblasts. Although stimulation of the fibroblast cell line MRC-5 with transforming growth factor-β1 (TGF-β1) increased α-SMA, HB-EGF reduced expression. HB-EGF also strongly inhibited the increased expression of α-SMA due to TGF-β1. Because HB-EGF is a potent fibroblast mitogen and TGF-β is usually antiproliferative, this study suggests that HB-EGF may contribute to a local balance between fibroblast proliferation and differentiation into myofibroblasts during scarring.

Recently, we and others have begun to study the recently described mitogenic growth factor heparin-binding epidermal growth factor-like growth factor (HB-EGF) in experimental kidney disease (1–4). HB-EGF is a member of the epidermal growth factor (EGF) family (5,6) and is synthesized as a transmembrane precursor that is cleaved by an unknown protease to yield the mature protein of 75–86 amino acids (7). The heparin-binding domain is cationic and predominantly contained within an N-terminal hydrophilic region in the mature peptide, which is linked to a C-terminal EGF-like domain (5,8).

The importance of HB-EGF lies in (*1*) the rapid induction of mRNA transcript numbers by various stimuli in several cell types, including endothelial cells, smooth muscle cells, and mesangial cells (2–4,6,9,10); (*2*) regulation by factors considered important in disease pathogenesis, including shear stress in human endothelial cells (11), angiotensin II in rat smooth muscle cells (12), and endothelin-1 in rat mesangial cells (4); and (*3*) evidence for multiple actions, including mitogenesis (5), chemotaxis (13), and cell adhesion (14).

In the course of studies designed to determine whether HB-EGF was upregulated in the remnant kidney model, we noted strikingly increased staining in the area surrounding the infarcted kidney (the peri-infarct area). Because HB-EGF has also been detected in cutaneous wound fluids from pigs and human burn victims (15,16), this observation suggested an important role for this fibroblast mitogen in tissue scarring and healing. Therefore, in this study we attempted to determine the distribution and function of HB-EGF in renal infarction.

Materials and Methods

Disease Model and Experimental Protocol

In the initial model, the purpose of which was to induce hypertrophy and hyperfiltration injury in the remnant kidney, 45 male Sprague

Received July 17, 1997. Accepted February 6, 1998.
This work was presented in part at the 29th Annual Meeting of the American Society of Nephrology, November 1996, and published in abstract form (*J Am Soc Nephrol* 7: 1858, 1996).
Correspondence to Dr. David Power, Department of Clinical Immunology, St. Vincent's Hospital, 41 Victoria Parade, Fitzroy 3065, Victoria, Australia.
1046-6673/0908-1464$03.00/0
Journal of the American Society of Nephrology

Dawley rats weighing 150 to 200 g at the start of the experiment were studied. In 24 rats (OP group), infarction of two-thirds of the left kidney was achieved by ligation of the two anterior extrarenal branches of the main renal artery leaving the proximal posterior branch to perfuse the upper pole, and a right total subcapsular nephrectomy was performed under anesthesia with intraperitoneal pentobarbitone (0.1 ml/100 g). In the control group of 17 rats (SHAM group), a sham operation was performed that comprised laparotomy and manipulation of the renal pedicles. Four rats died intraoperatively, and one each from the SHAM and OP groups died postoperatively. Rats were sacrificed at days 1, 3, and 5 and at weeks 1, 2, 3, and 4, and the kidneys were harvested. In an additional group of 10 rats, 2/6 nephrectomy was performed (*i.e.*, the contralateral kidney was not removed). Kidneys were harvested at some of the same time points as noted for the remnant kidney model.

In Situ Hybridization

A rat HB-EGF cDNA probe corresponding to positions 231 to 254 and 707 to 726, respectively, in the published sequence of rat cDNA (17), was produced by PCR amplification, as described previously (2). Primers were selected to include the sequence encoding the mature HB-EGF protein. This 495-bp cDNA fragment was subcloned into the multiple cloning site of the plasmid pGEM-T (Promega, Madison, WI) between the SP6 and T7 promoters. The insert was sequenced over its full length on both strands and found to be identical to the published sequence of rat HB-EGF. pGEM-T containing the HB-EGF cDNA fragment was linearized with the restriction enzyme *Sac*II (sense probe) or *Spe*I (antisense probe). Labeled riboprobes were synthesized using T7 RNA polymerase (antisense probe) or SP6 RNA polymerase (sense probe) incorporating digoxigenin-labeled uridine-triphosphate (Boehringer Mannheim, Mannheim, Germany). The antisense riboprobe, but not the sense riboprobe, detected a 2.5-kb transcript on a Northern blot of mesangial cell RNA. Paraffin sections were cut 4-μm-thick. Sections were dewaxed in xylene and dehydrated in alcohol, treated with 0.2 M HCl for 20 min, rinsed with diethyl pyrocarbonate (DEPC) water twice for 5 min, then placed in 2× SSC at 70°C for 10 min and rinsed in DEPC water. Digestion of sections was undertaken with 20 μg/ml proteinase K (Sigma Chemical Co., Castle Hill, NSW, Australia) in 100 mM Tris-HCl (pH 8.0)/50 mM ethylenediaminetetra-acetic acid (EDTA) at 37°C for 30 min. Digestion was stopped by immersion in 2 mg/ml glycine in phosphate-buffered saline (PBS). Slides were rinsed in PBS twice and fixed in 4% paraformaldehyde for 15 min, rinsed with PBS, and equilibrated with 100 mM triethanolamine, pH 8.0. Acetic anhydride was added to block positively charged groups that might bind the probe. Sections were prehybridized in hybridization buffer (50% formamide, 5× SSC, 2% block reagent [Boehringer Mannheim], 0.02% sodium dodecyl sulfate [SDS], and 0.1% *N*-lauroylsarcosine) for 60 min at 37°C and then hybridized overnight with denatured digoxigenin-labeled sense and antisense riboprobe at a concentration of 150 ng/ml in a humidified chamber at 42°C. After treatment of the slides with DNase-free RNase A (5 μg/ml) for 30 min at 37°C, colorimetric detection of mRNA after hybridization was accomplished with the nonradioactive nucleic acid detection kit (Boehringer Mannheim) according to the manufacturer's instructions. Sections were counterstained with Nuclear Fast Red. Tissue obtained from each of three rats was stained and examined at each time point.

Immunohistochemical Staining to Detect α-Smooth Muscle Actin

Tissue blocks were immersion-fixed in 4% paraformaldehyde and embedded in paraffin. Paraffin sections 4 μm thick were cut on a microtome and dried overnight at 37°C. Sections were dewaxed, and endogenous peroxidase activity was inhibited using 3% hydrogen peroxide for 10 min. Sections were then blocked with sheep serum (Life Technologies, Gaithersburg, MD) for 30 min and incubated overnight at 4°C with anti-α-smooth muscle actin (α-SMA) monoclonal antibody (mAb) 1A4 from Sigma (18). Negative control was an isotype-matched mAb. Antibody binding was detected using a triple-layer technique, comprising rabbit anti-mouse Ig diluted 1:50 (Dako, Carpinteria, CA) followed by mouse peroxidase antiperoxidase (Dako) diluted 1:100, each for 30 min, with washing steps between incubations. Sections were developed using nickel-enhanced diaminobenzidine (Pierce, Rockford, IL) and counterstained with hematoxylin.

Localization of Tubular Staining Using Tubular Markers

To determine the location of tubular staining with anti-HB-EGF antibodies, tubular markers were used, as described by Nadasdy *et al.* (19). Sequential sections were stained with fluorescein-labeled lectins (Sigma) to identify distal convoluted tubules and collecting ducts (*Arachis hypogaea*) and proximal renal tubules (*Phaseolus vulgaris* erythroagglutinin). Lectin staining was identified using immunoperoxidase-conjugated anti-FITC Fab fragments (Boehringer Mannheim), followed by diaminobenzidine and hematoxylin as described earlier. Rabbit anti-Tamm-Horsfall antibody, a generous gift of Dr. H. Y. Lan (Monash Medical Centre, Clayton, Victoria, Australia), was used to identify cortical and medullary thick ascending limbs of the loop of Henle (TAL). Antibody binding was detected using a rabbit peroxidase antiperoxidase assay (Dako).

Terminal deoxynucleotidyl transferase-mediated nick end labeling (TUNEL) staining to detect apoptotic cells was performed using a published method (20). Briefly, neutral-buffered formalin-fixed, paraffin-embedded tissue was dewaxed and rehydrated. Sections were treated with proteinase K and, after washing, incubated with biotin-labeled dUTP. Binding was detected by the avidin-biotin-complex method, using the ABC Elite kit (Vector Laboratories, Burlingame, CA). Sections were counterstained in Harris hematoxylin.

Northern Blot Analysis

Kidneys were homogenized in Trizol reagent (Life Technologies, Grand Island, NY), using a pro200 homogenizer (Proscientific, Inc., Monroe, CT), according to the manufacturer's instructions. Thereafter, 1/5 vol of chloroform was added to the sample, incubated for 5 min at room temperature, then centrifuged at 12,000 × *g*, 4°C for 15 min. The upper aqueous phase was removed and precipitated with an equal volume of isopropanol, incubated at room temperature for 5 min, and then centrifuged at 12,000 × *g*, 4°C for 10 min. The pellet was washed twice with 75% ethanol and centrifuged at 8000 × *g*, 4°C for 5 min. The pellet was then air-dried and dissolved in DEPC-treated water, and the RNA was used for Northern analysis. RNA samples were electrophoresed on 1% agarose gels containing 7.2% formaldehyde and transferred to nylon membranes (GeneScreen Plus, Dupont). RNA was fixed using a Stratalinker (Stratagene, La Jolla, CA), and the membranes were prehybridized in hybridization solution (5× saline-sodium phosphate-EDTA, 5× Denhardt's, 0.5% SDS, 50% formamide, and 100 μg/ml sheared herring sperm DNA) for 4 h at 42°C, after which 2 × 10^6 counts/ml denatured ^{32}P-labeled HB-EGF insert was added and incubated overnight. Membranes were then sequentially washed with 2× SSC/0.1% SDS, 1× SSC/0.1% SDS, and 0.1× SSC/0.1% SDS for 15 min at 42°C. Filters were then exposed to x-ray film at −70°C. Membranes were then hybridized

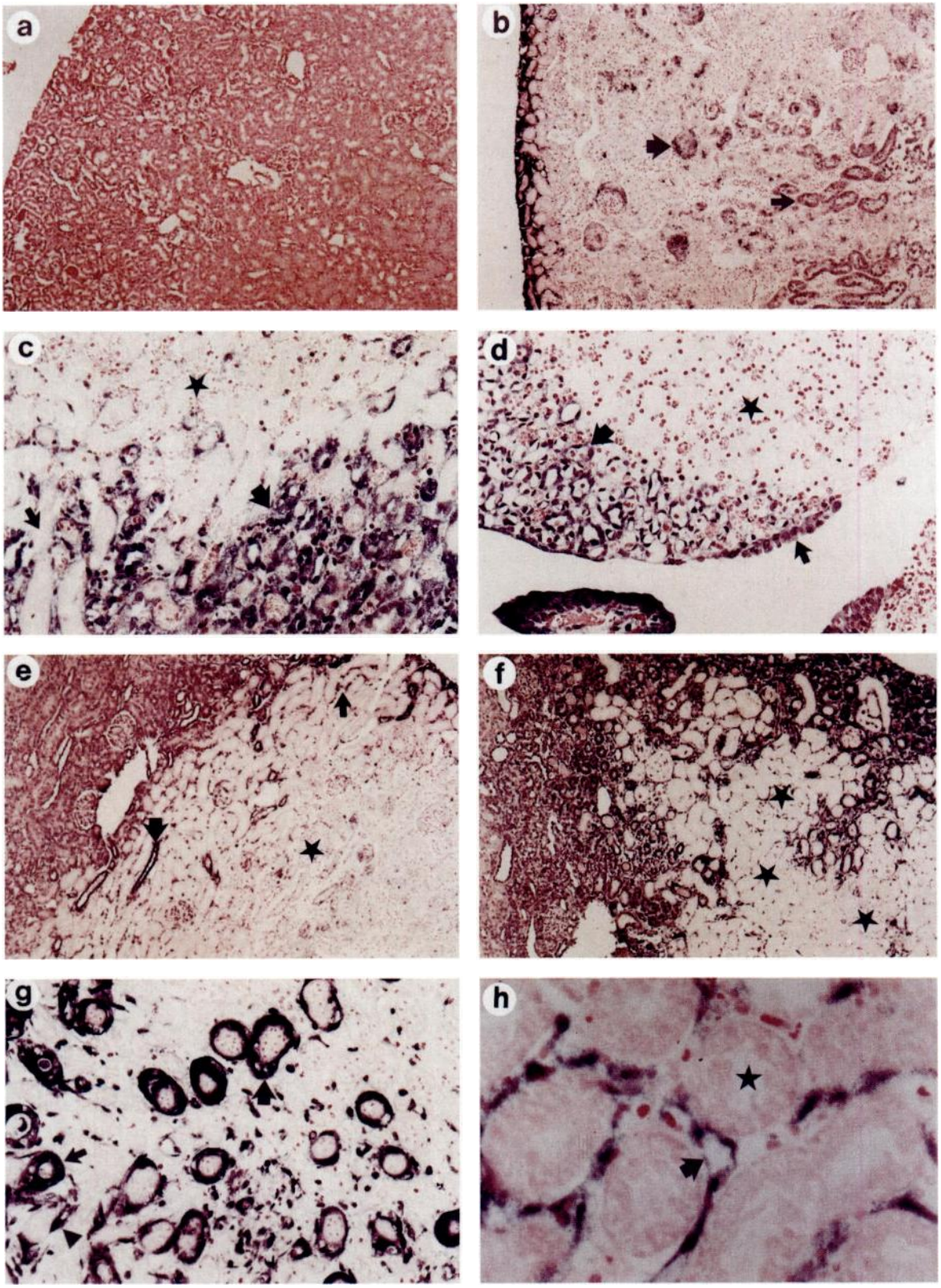

Figure 1. (a through h) *In situ* hybridization using antisense heparin-binding epidermal growth factor-like growth factor (HB-EGF) riboprobe. (a) Normal kidney with almost no staining. (b) Infarcted kidney at 24 h, showing prominent staining in the pericapsular area, to the left. There is also some staining in necrotic tubules (thin arrow) and glomeruli (thick arrow). (c) Higher power magnification of the perinecrotic area at day 1, showing upregulation of HB-EGF mRNA by most of the viable tubules. The middle of the necrotic area is marked (★). (d) Section taken from the papilla at day 1, showing expression by urothelium (thin arrow) and tubules (thick arrow). The necrotic area is marked (★). (e) At day 3 postinfarction, there is a generalized increase in tubular staining abutting the infarcted area (★), together with intense staining of a few viable tubules within the infarcted area (thick arrow). Between necrotic tubules, some positive cells are seen (thin arrow), which may be endothelial

with GAPDH as above. Quantification of signals was performed by densitometry (Molecular Dynamics Computing Densitometer, model 300A) using ImageQuant Software, version 3.0. Values for each sample were expressed as the ratio of HB-EGF signal to GAPDH signal.

In Vitro Stimulation of Fibroblasts and Detection of α-SMA

These experiments were based on studies reported previously by Gabbiani and coworkers (21). The fetal lung fibroblast cell line MRC-5 was obtained from American Type Culture Collection (Rockville, MD) and used between passages 5 and 7 after thawing. Cells were plated in 6-well tissue culture plates at 2×10^4 cells per well in RPMI containing 15% fetal calf serum. The medium was changed 24 h later and the following recombinant human growth factors (R&D Systems, Minneapolis, MN) were used: 10 ng/ml HB-EGF, 5 ng/ml TGF-β, and 10 ng/ml platelet-derived growth factor-BB (PDGF-BB). All experiments were performed six times and each was analyzed separately. After 5 d, the cells were washed twice with normal saline and lysed with 100 μl of lysis buffer per well (50 mM Tris-HCl, pH 7.5, 150 mM NaCl, 5 mM EDTA, 0.5% Triton X-100, 10 μg/ml leupeptin, 1.5 mM phenylmethylsulfonyl fluoride, and 10 μg/ml aprotinin) for 30 min at 4°C. Lysed cells were then removed using a cell scraper and centrifuged at 15,000 rpm at 4°C for 5 min to remove nuclei. Protein concentrations were measured using the BioRad Protein Standard Assay (BioRad Laboratories, Regents Park, NSW, Australia). The lysates were aliquoted, mixed with reducing buffer, and stored at −70°C. For Western blots, 20 μg of protein was run on a 12.5% SDS-polyacrylamide gel electrophoresis gel and transferred to nitrocellulose using the Bio-Rad Minigel apparatus. Blots were blocked with 5% skim milk powder in Tris-buffered saline, then incubated for 60 min with a monoclonal anti-α-SMA antibody (18), supplied by Sigma, and diluted 1:4000. After washing with 0.5% Tween 20 in Tris-buffered saline, the blots were probed with horseradish peroxidase-conjugated rabbit anti-mouse antibody (Dako) diluted 1:2000 for 30 min. Antibody binding was detected using the Pierce Super-Signal System (Pierce). For Coomassie blue-stained gels, 10 μg of lysate was added per lane. Molecular sizes were calculated using High Molecular Weight Rainbow Markers (Amersham PLC, Bucks, United Kingdom). Signals were quantified by densitometry using Molecular Dynamics Computing Densitometer and ImageQuant Software, as described previously.

Statistical Analyses

Statistical analyses were performed using the Instat software package, version 2.01, from GraphPad Software. Multiple comparisons were performed using ANOVA, followed by the Tukey–Kramer multiple comparison test (for equal variances) or Dunn multiple comparison test (for unequal variances). A P value < 0.05 was considered significant.

Results

Distribution of HB-EGF in Normal Kidney

In the normal rat kidney, HB-EGF mRNA transcripts were almost undetectable by *in situ* hybridization (Figure 1a).

HB-EGF mRNA in Renal Infarction

Twenty-four hours after ligation of the upper and lower pole branches of the renal artery, necrotic tubular cells were identified by their pyknotic nuclei or loss of nuclei and clumping of the cytoplasm. The most striking feature of the *in situ* hybridization studies was the marked expression of HB-EGF mRNA in the peri-infarct area from day 1 onward (Figure 1, b through d). Initially, this occurred in most tubular cells bordering the necrotic area, including those in the papilla (Figure 1d), as well as the urothelium (Figure 1d) and overlying capsular fibroblasts (Figure 1b).

At day 3, tubular expression was more intense (Figure 1e). Endothelial cells of some small arteries and venules were strongly positive at day 3, and there was expression by cells bordering necrotic tubules that were probably endothelial cells of the peritubular capillaries (Figure 1e). At this time, and increasing at day 5, the peri-infarct area was found to contain large areas of spindle-shaped cells that expressed α-SMA (Figure 2b), which was not present in normal kidney (Figure 2a). These cells were difficult to distinguish from endothelial cells except by staining with α-SMA antibody. Electron microscopy of sections taken at day 5, together with their spindle shape and reactivity with the mAb against α-SMA, suggested that they were myofibroblasts (22).

At day 5, staining for HB-EGF mRNA in the peri-infarct area was at its most intense (Figure 1f), with some tubular islands in the necrotic area staining strongly for HB-EGF mRNA (Figure 1g). Some of these tubules were surrounded by a layer of cells that also expressed HB-EGF mRNA very strongly. In some sections, cells expressing α-SMA (presumed myofibroblasts) were seen directly apposed to tubules that strongly expressed HB-EGF mRNA (Figure 2, c and d). Some of the presumed myofibroblasts were in areas that were strongly positive for HB-EGF mRNA (Figure 2, c and d). It was impossible, however, to identify individual myofibroblasts in sequential sections. At this stage, too, endothelial cells in arterioles bordering the necrotic area (Figure 2, e and f) as well as capillary endothelial cells were strongly positive (Figure 1h). Glomeruli bordering or within the infarcted area expressed HB-EGF mRNA mainly in visceral and parietal glomerular epithelial cells (Figure 2, g and h).

At day 7 and later, there was a gradual reduction in HB-EGF expression in all areas. By week 4, expression was back to levels seen in normal kidneys. The only evidence of infarction was a distortion of tissue architecture at the poles of the kidneys and some continued expression of α-SMA in these areas.

These results were confirmed by Northern blots of RNA obtained from tissue removed from the peri-infarcted region (Figure 3). One-way ANOVA showed a highly significant difference between treatment groups ($P < 0.0001$). There was

cells. (f) Maximal staining intensity of tubules bordering the necrotic area (★) at day 5. (g) Higher power magnification of HB-EGF mRNA expression by isolated tubular elements (thin arrow), cells surrounding necrotic tubules (thick arrow), and endothelial cells (arrowhead) at day 5 within a predominantly necrotic area. (h) Higher power magnification showing expression by endothelial cells (thick arrow) surrounding necrotic tubules (★) at day 5. Magnification: ×25 in a, b, e, and f; ×50 in d; ×75 in c and g; and ×200 in h.

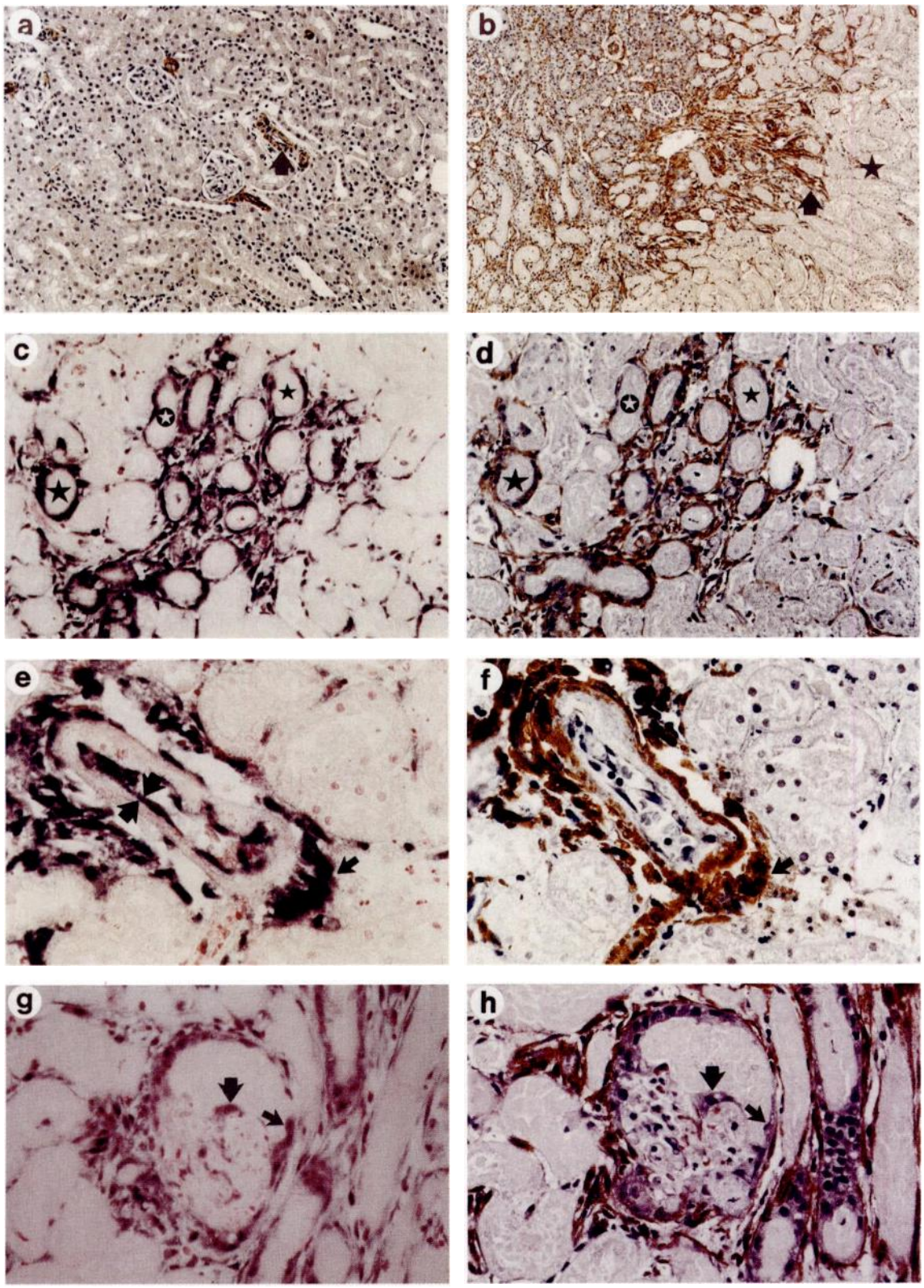

Figure 2. (a through h) *In situ* hybridization for HB-EGF mRNA and immunohistochemical staining for α-smooth muscle actin (α-SMA). (a) Staining for α-SMA in normal kidney is present mainly within the media of arteries and arterioles (thick arrow) (×50). (b) At day 5 postinfarction, spindle-shaped cells expressing α-SMA (thick arrow) are seen extending into the necrotic area on the right (★), and surrounding tubules in the viable area on the left. (×25). Sections c and d are sequential and can be aligned using the symbols ★, ⋆, and ✪, which correspond to the same tubular cross sections (×75). (c) *In situ* hybridization showing expression of HB-EGF mRNA by cells surrounding necrotic tubules (⋆ and ✪), as well as some viable tubular cells (★). (d) Sequential section stained for α-SMA showing spindle-shaped cells surrounding necrotic tubules. Sections e and f are sequential (×100). (e) HB-EGF mRNA expression by endothelial cells (two thick arrows) and cells surrounding an arteriole (thin arrow) within a necrotic area. (f) α-SMA expression in a sequential

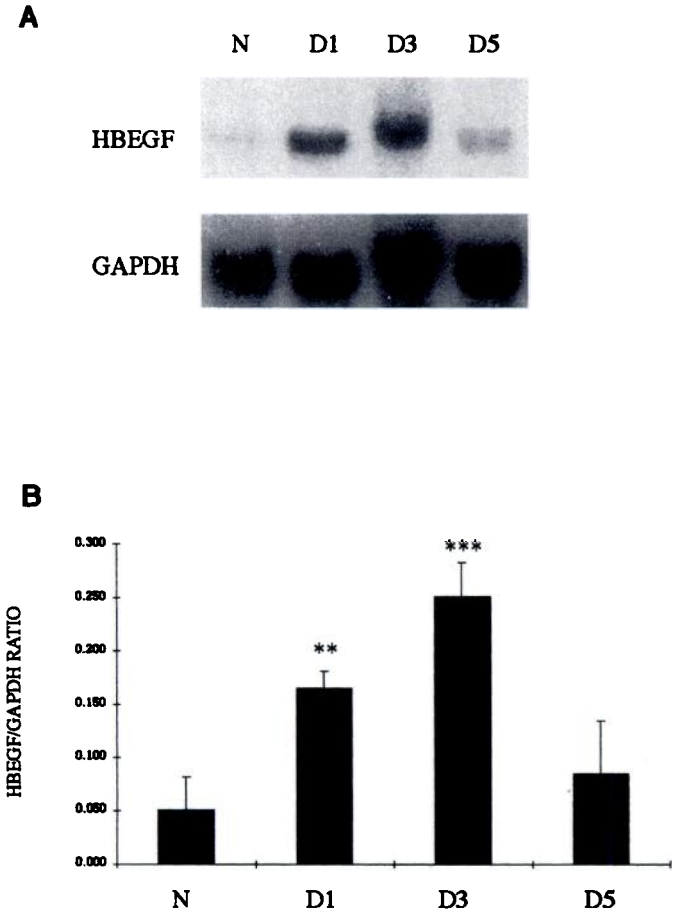

Figure 3. (A) Northern blot of total RNA from normal kidney and the peri-infarct areas of kidneys removed at days 1, 3, and 5 postinfarction. A 2.5-kb band is detected with the HB-EGF cDNA probe corresponding to the expected size of HB-EGF. GAPDH is used as a loading control. (B) Ratios of signals obtained with HB-EGF cDNA probe compared to those with GAPDH ($n = 4$). Results are expressed as mean ± 1 SD. $^{**}P < 0.01$; $^{***}P < 0.001$.

a statistically significant increase in HB-EGF mRNA, expressed as HB-EGF/GAPDH densitometric ratios, at days 1 (threefold increase; $P < 0.01$; Tukey–Kramer multiple comparison test) and 3 (fivefold increase; $P < 0.001$), but not at day 5, although mean ratios were higher at this time point than in the controls (Figure 3).

Tubular Expression of HB-EGF in the Peri-Infarct Region

To define the tubules that express HB-EGF mRNA in the peri-infarct region, sequential sections from day 5 were stained immunohistochemically with tubular markers and by *in situ* hybridization for HB-EGF mRNA. Unfortunately, tubules along the ischemic edge of the tissue were usually negative for all of the markers. However, it was possible to identify some cells of the TAL and cells of the distal convoluted tubules and cortical collecting ducts, which were positive for HB-EGF (Figure 4).

Identification of Apoptotic Cells in the Infarcted and Peri-Infarct Areas

In view of evidence that apoptosis may contribute to cell loss in some ischemic conditions and the possibility that HB-EGF expression may be altered in areas where cell loss was primarily due to apoptosis, sections were stained using the TUNEL technique and examined by electron microscopy for evidence of apoptosis. Although large parts of the necrotic area had pyknotic nuclei, these were not typical, morphologically, of apoptotic cells by electron microscopy and did not stain using the TUNEL technique. Few typical apoptotic cells were seen, apart from day 5 when 1.1 ± 0.2 cells per tubular cross section were apoptotic in tubules bordering the peri-infarct area.

Effect of HB-EGF on Expression of α-SMA by Cultured Fibroblasts

Because HB-EGF mRNA was expressed by tubules that were surrounded by myofibroblasts, and probably by myofibroblasts themselves, studies were performed to determine whether HB-EGF increases expression of α-SMA by the human fibroblast cell line MRC-5. Fibroblasts were incubated with growth factors for 5 d before harvesting and analysis by Western blot for α-SMA protein. Expression of α-SMA protein in cultures treated with growth factors was compared with untreated cells grown in 15% fetal calf serum in RPMI (Figure 5). Bartlett's test showed a highly significant difference in the SD of the six groups ($P < 0.0001$), so nonparametric statistics were used. ANOVA (Kruskall–Wallis nonparametric ANOVA) showed a highly significant difference between the medians of the six primary treatment groups ($P < 0.0001$). Treatment of MRC-5 cells with HB-EGF reduced median levels of α-SMA expression from 422 (range, 227 to 764) densitometric units to 45 (range, 0 to 67), an 89% reduction ($P < 0.05$, Dunn multiple comparison test), whereas TGF-β increased it by 196% to 826 (range, 300 to 1643), although this was not significant. When HB-EGF was added to TGF-β, there was an 85% reduction in the level of α-SMA compared with TGF-β alone, but this was not significant. PDGF alone had little effect.

Discussion

HB-EGF is a very potent fibroblast mitogen that has previously been reported to constitute >50% of the heparin-binding mitogenic activity for fibroblasts in skin wound fluids (15,16) and to be present in the epithelium and sweat glands in partial

section demonstrating expression by cells surrounding an arteriole (thin arrow) in a similar distribution to HB-EGF mRNA. Endothelial cells are negative for α-SMA. Sections g and h are sequential (×100). (g) *In situ* hybridization for HB-EGF in a glomerulus within a necrotic area at day 5, showing strong expression by visceral (thick arrow) and parietal (thin arrow) glomerular epithelial cells. (h) The sequential section stained with α-SMA, showing no expression by glomerular epithelial cells identified by arrows in the previous section.

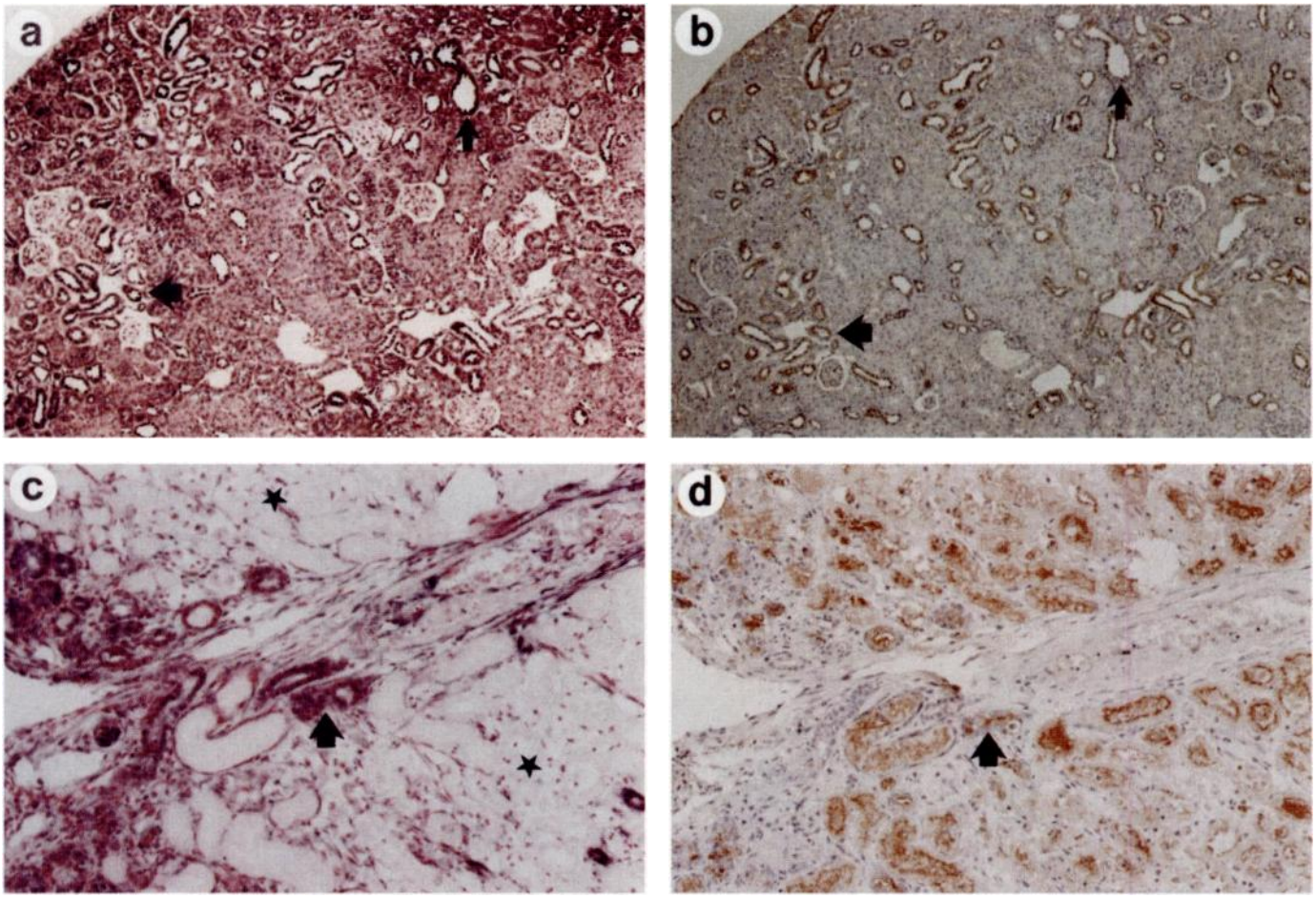

Figure 4. (a through d) Staining of sequential sections for HB-EGF, by *in situ* hybridization, and tubular markers, by immunohistochemistry. Sections a and b are sequential (×25). (a) *In situ* hybridization for HB-EGF of an area bordering the necrotic area, which is at the bottom right of the photomicrograph. Strongly positive tubules are shown by thick and thin arrows. (b) Sequential section stained using the FITC-labeled lectin *Arachis hypogaea*, a marker for distal convoluted tubules and collecting ducts, showing staining of some of the same tubules as in the previous section (thick and thin arrows). Sections c and d are sequential (×50). (c) *In situ* hybridization for HB-EGF within a necrotic area (★) showing strong staining of a number of tubules, including one (thick arrow) which, on the sequential section (d) stained with anti-Tamm-Horsfall antibody, was positive (thick arrow). A number of other tubules that were apparently positive were probably nonspecifically stained, because most of the immunoreactivity was within the lumen.

thickness burns (16). This study demonstrates striking expression of HB-EGF by renal tubules, endothelial cells, urothelium, and myofibroblasts in the area surrounding a renal infarct. Increased expression was confirmed by Northern blot analysis, which showed a maximal fivefold increase at day 3, postinfarction. The apparent discrepancy between Northern blots and *in situ* hybridization, in which the most intense expression was seen at day 5, could be due to a more localized increase at day 5 than at day 3. Expression changed during the course of the model so that, at 24 h, the most prominent staining was seen in the tubules, whereas endothelial cells and cells surrounding necrotic tubules (probably myofibroblasts) were more positive over succeeding days. Tubular expression has previously been reported in the ischemia-reperfusion model of renal injury, where it was found predominantly in tubules of the thick ascending limb of the loop of Henle in the inner stripe of the outer medulla (1). In the present study, most tubules bordering the infarcted area appeared to express HB-EGF mRNA, including those in the papilla. However, it was not possible to stain most of these with tubular markers, so we could not accurately identify all tubular segments expressing HB-EGF. Distal convoluted tubules, cortical collecting ducts, and TAL, however, were clearly identified as positive.

Endothelial cell expression of HB-EGF mRNA has been reported in cells isolated from regenerating livers (23) and in cells overlying areas of myointimal hyperplasia induced, in rats, by balloon injury of carotid arteries (24). In this study, microvascular endothelial cell expression of HB-EGF was first definitely observed 3 d after ligation of the renal arteries at the margin of the area of necrosis. Endothelial cells in larger arterioles bordering the necrotic area also became positive by *in situ* hybridization at day 5.

Cells appearing to be myofibroblasts, based on their spindle shape and expression of α-SMA, first appeared at day 3 after infarction in the peri-infarct zone. Staining of sequential sections showed that morphologically similar cells in these loca-

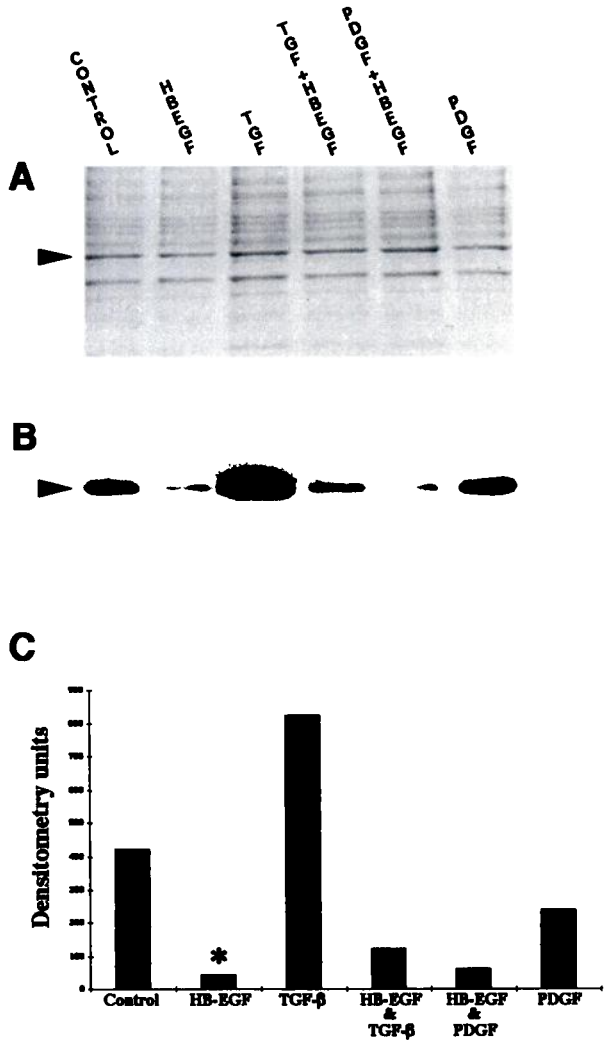

Figure 5. Western blot of MRC-5 cell lysates, probed with anti-α-SMA mAb. (A) Coomassie-stained gel showing approximate equivalence of total actin in each of the lanes (arrowhead). (B) Western blot probed with α-SMA mAb showing variable expression of the α-SMA isoform, despite equivalent staining for total actin. (C) Median values for α-SMA expression, expressed in densitometric units, in Western blots from six experiments. Results obtained from cells treated with HB-EGF, transforming growth factor-β (TGF-β), HB-EGF + TGF-β, HB-EGF + platelet-derived growth factor (PDGF), and PDGF were compared with the untreated control by the Dunn multiple comparison test. $*P < 0.05$.

tions were also positive for HB-EGF mRNA, although it proved impossible to identify individual cells in these sections.

The presence of HB-EGF in areas of tissue damage suggests that it may be important in wound healing and scarring. As a heparin-binding fibroblast mitogen, it clearly has the potential to stimulate long-term fibroblast proliferation. In this study, cells with the characteristics of myofibroblasts were present around tubules that were strongly positive for HB-EGF mRNA. It seemed possible, therefore, that HB-EGF contributed to the switch to the myofibroblast phenotype. It was surprising, in the event that HB-EGF actually reduced expression of α-SMA by the fibroblast cell line MRC-5. It also inhibited the effect of TGF-β, which has previously been reported to increase α-SMA in fibroblasts (21).

HB-EGF is a potent fibroblast mitogen, whereas TGF-β is usually antiproliferative (25,26). The balance between fibroblast proliferation and transformation to the more differentiated phenotype may be controlled, therefore, by the balance between these two growth factors. A potential benefit to tubular cells expressing HB-EGF is that they may reduce local myofibroblast transformation and, therefore, prevent distortion of viable cellular architecture in areas that undergo contraction during scarring. Although it is difficult to understand why cells that have acquired the myofibroblast phenotype and strongly express α-SMA might possess mRNA for a growth factor that inhibits expression of α-SMA, this probably reflects the complexity of gene regulation in this situation and the involvement of other, unrecognized factors.

A second possible role for HB-EGF is in angiogenesis. Although HB-EGF is not mitogenic for human umbilical vascular endothelial cells (5), there is an isolated report of its ability to induce angiogenesis in human microvascular endothelial cells (27). HB-EGF produced by cells in the area surrounding infarction, therefore, may contribute to the formation of new capillaries during healing and scar formation.

The possible function of HB-EGF production by the endothelial cells of larger arterioles and arteries is less obvious. In other locations, HB-EGF is considered to be a potential contributor to the pathogenesis of atherosclerosis because it is mitogenic and chemotactic for smooth muscle cells (5,13), increases production of fibroblast growth factor-2 by these cells (28), and upregulates expression of receptors such as the macrophage colony-stimulating factor receptor (c-fms) and the scavenger receptor for cholesterol (29). These actions tend to increase smooth muscle cell numbers and contribute to their migration into the intima. This could also occur as a physiologic response to tissue injury so that, in arteries bordering an area of infarcted tissue, endothelial cell production of HB-EGF leads to migration and proliferation of smooth muscle cells from the media and obliteration of the arterial lumen.

The stimulus to HB-EGF expression in the peri-infarct area is unknown. One obvious possibility is a period of transient ischemia followed by reperfusion. In studies of a tubular cell line, Homma *et al.* (1) reported that both hypoxia and reoxygenation increased HB-EGF mRNA, although reoxygenation was more effective. In the rat model of renal ischemia-reperfusion injury, in which the ischemic period was 40 min, HB-EGF levels were elevated for 6 h after reperfusion and, in some instances, for up to 24 to 48 h (1). In that study, however, expression was restricted to a subset of tubular cells and was not reported in endothelial cells. A second possibility is that the necrotic cells have leaked some factor that leads to long-term increases in HB-EGF mRNA expression by a variety of cell types, including tubular cells at all levels and endothelial cells. At present there is no evidence of such a factor.

In conclusion, this study shows that HB-EGF mRNA is produced by a variety of cell types in the area surrounding renal infarction. Although we have not yet demonstrated synthesis of HB-EGF protein by these cells, the multiple actions of

HB-EGF *in vitro* predict a complex role for HB-EGF in the process of scarring. The interaction of HB-EGF with other growth factors is likely to be very important in directing the response to tissue injury.

Acknowledgments

Drs. Kirkland and Paizis are recipients of postgraduate scholarships from the National Health and Medical Research Council of Australia. This work was supported by a grant from the National Health and Medical Research Council of Australia to Dr. Power. We are grateful to Tim Hewitson of the Department of Nephrology at the Royal Melbourne Hospital for performing the TUNEL staining.

References

1. Homma T, Sakai M, Cheng HF, Yasuda T, Coffey RJJ, Harris RC: Induction of heparin-binding epidermal growth factor-like growth factor mRNA in rat kidney after acute injury. *J Clin Invest* 96: 1018–1025, 1995
2. Polihronis M, Murphy BF, Pearse MJ, Power DA: Heparin-binding epidermal growth factor-like growth factor, an immediate-early gene for mesangial cells, is up-regulated in the Thy-1.1 model. *Exp Nephrol* 4: 271–278, 1996
3. Tan MS, Lee YJ, Shin SJ, Tsai JH: Regulation of heparin binding-epidermal growth factor-like growth factor gene expression by LDL and oxidized-LDL in rat mesangial cells. *Biochem Biophys Res Commun* 202: 1001–1008, 1994
4. Tan MS, Tsai JC, Lee YJ, Chen HC, Shin SJ, Lai YH, Perrella MA, Bianchi C, Higashiyama S, Endege W: Induction of heparin-binding epidermal growth factor-like growth factor mRNA by protein kinase C activators. *Kidney Int* 46: 690–695, 1994
5. Higashiyama S, Abraham JA, Miller J, Fiddes JC, Klagsbrun M: A heparin-binding growth factor secreted by macrophage-like cells that is related to EGF. *Science* 251: 936–939, 1991
6. Fen Z, Dhadly MS, Yoshizumi M, Hilkert RJ, Quertermous T, Eddy RL, Shows TB, Lee ME: Structural organization and chromosomal assignment of the gene encoding the human heparin-binding epidermal growth factor-like growth factor/diphtheria toxin receptor. *Biochemistry* 32: 7932–7938, 1993
7. Higashiyama S, Lau K, Besner GE, Abraham JA, Klagsbrun M: Structure of heparin-binding EGF-like growth factor: Multiple forms, primary structure, and glycosylation of the mature protein. *J Biol Chem* 267: 6205–6212, 1992
8. Thompson SA, Higashiyama S, Wood K, Pollitt NS, Damm D, McEnroe G, Garrick B, Ashton N, Lau K, Hancock N: Characterization of sequences within heparin-binding EGF-like growth factor that mediate interaction with heparin. *J Biol Chem* 269: 2541–2549, 1994
9. Nakano T, Raines EW, Abraham JA, Wenzel FG, Higashiyama S, Klagsbrun M, Ross R: Glucocorticoid inhibits thrombin-induced expression of platelet-derived growth factor A-chain and heparin-binding epidermal growth factor-like growth factor in human aortic smooth muscle cells. *J Biol Chem* 268: 22941–22947, 1993
10. Pan Z, Kravchenko VV, Ye RD: Platelet-activating factor stimulates transcription of the heparin-binding epidermal growth factor-like growth factor in monocytes: Correlation with an increased kappa B binding activity. *J Biol Chem* 270: 7787–7790, 1995
11. Morita T, Yoshizumi M, Kurihara H, Maemura K, Nagai R, Yazaki Y: Shear stress increases heparin-binding epidermal growth factor-like growth factor mRNA levels in human vascular endothelial cells. *Biochem Biophys Res Commun* 197: 256–262, 1993
12. Temizer DH, Yoshizumi M, Perrella MA, Susanni EE, Quertermous T, Lee ME: Induction of heparin-binding epidermal growth factor-like growth factor mRNA by phorbol ester and angiotensin II in rat aortic smooth muscle cells. *J Biol Chem* 267: 24892–24896, 1992
13. Higashiyama S, Abraham JA, Klagsbrun M: Heparin-binding EGF-like growth factor stimulation of smooth muscle cell migration: Dependence on interactions with cell surface heparan sulfate. *J Cell Biol* 122: 933–940, 1993
14. Das SK, Wang XN, Paria BC, Damm D, Abraham JA, Klagsbrun M, Andrews GK, Dey SK: Heparin-binding EGF-like growth factor gene is induced in the mouse uterus temporally by the blastocyst solely at the site of its apposition: A possible ligand for interaction with blastocyst EGF-receptor in implantation. *Development* 120: 1071–1083, 1994
15. Marikovsky M, Breuing K, Liu PY, Eriksson E, Higashiyama S, Farber P, Abraham J, Klagsbrun M: Appearance of heparin-binding EGF-like growth factor in wound fluid as a response to injury. *Proc Natl Acad Sci USA* 90: 3889–3893, 1993
16. McCarthy DW, Downing MT, Brigstock DR, Luquette MH, Brown KD, Abad MS, Besner GE: Production of heparin-binding epidermal growth factor-like growth factor (HB-EGF) at sites of thermal injury in pediatric patients. *J Invest Dermatol* 106: 49–56, 1996
17. Abraham JA, Damm D, Bajardi A, Miller J, Klagsbrun M, Ezekowitz RA: Heparin-binding EGF-like growth factor: Characterization of rat and mouse cDNA clones, protein domain conservation across species, and transcript expression in tissues. *Biochem Biophys Res Commun* 190: 125–133, 1993
18. Skalli O, Ropraz P, Trzeciak A, Benzonana G, Gillessen D, Gabbiani G: A monoclonal antibody against alpha-smooth muscle actin: A new probe for smooth muscle differentiation. *J Cell Biol* 103: 2787–2796, 1986
19. Nadasdy T, Laszik Z, Blick KE, Johnson DL, Burst-Singer K, Nast C, Cohen AH, Ormos J, Silva FG: Human acute tubular necrosis: A lectin and immunohistochemical study. *Hum Pathol* 26: 230–239, 1995
20. Smith KG, Hewitson TD, Nossal GJ, Tarlinton DM: The phenotype and fate of the antibody-forming cells of the splenic foci. *Eur J Immunol* 26: 444–448, 1996
21. Desmouliere A, Geinoz A, Gabbiani F, Gabbiani G: Transforming growth factor-beta 1 induces alpha-smooth muscle actin expression in granulation tissue myofibroblasts and in quiescent and growing cultured fibroblasts. *J Cell Biol* 122: 103–111, 1993
22. Schmitt-Graff A, Desmouliere A, Gabbiani G: Heterogeneity of myofibroblast phenotypic features: An example of fibroblastic cell plasticity [Review]. *Virchows Arch* 425: 3–24, 1994
23. Kiso S, Kawata S, Tamura S, Higashiyama S, Ito N, Tsushima H, Taniguchi N, Matsuzawa Y: Role of heparin-binding epidermal growth factor-like growth factor as a hepatotrophic factor in rat liver regeneration after partial hepatectomy. *Hepatology* 22: 1584–1590, 1995
24. Igura T, Kawata S, Miyagawa J, Inui Y, Tamura S, Fukuda K, Isozaki, Yamamori K, Taniguchi N, Higashiyama S, Matsuzawa Y: Expression of heparin-binding epidermal growth factor-like growth factor in neointimal cells induced by balloon injury in rat carotid arteries. *Arterioscler Thromb Vasc Biol* 16: 1524–1531, 1996
25. MacKay K, Striker LJ, Stauffer JW, Doi T, Agodoa LY, Striker GE: Transforming growth factor-beta: Murine glomerular receptors and responses of isolated glomerular cells. *J Clin Invest* 83: 1160–1167, 1989

26. Feng XH, Filvaroff EH, Derynck R: Transforming growth factor-beta (TGF-beta)-induced down-regulation of cyclin A expression requires a functional TGF-beta receptor complex: Characterization of chimeric and truncated type I and type II receptors. *J Biol Chem* 270: 24237–24245, 1995
27. Ushiro S, Ono M, Izumi H, Kohno K, Taniguchi N, Higashiyama S, Kuwano M: Heparin-binding epidermal growth factor-like growth factor: p91 activation induction of plasminogen activator/inhibitor, and tubular morphogenesis in human microvascular endothelial cells. *Jpn J Cancer Res* 87: 68–77, 1996
28. Peifley KA, Alberts GF, Hsu DK, Feng SL, Winkles JA: Heparin-binding epidermal growth factor-like growth factor regulates fibroblast growth factor-2 expression in aortic smooth muscle cells. *Circ Res* 79: 263–270, 1996
29. Inaba T, Ishibashi S, Harada K, Ohsuga J, Ohashi K, Yagyu H, Yazaki Y, Higashiyama S, Kawata S, Matsuzawa Y, Yamada N: Induction of macrophage colony-stimulating factor receptor (c-fms) expression in vascular medial smooth muscle cells treated with heparin binding epidermal growth factor-like growth factor. *J Biol Chem* 271: 24413–24417, 1996